Chapter 9

Getting a paleomagnetic direction

Suggested Reading

For background:
Chapter 4: Butler (1992)
To learn more:
Chapters 8, 9: Collinson (1983)

9.1 Introduction

As discussed in Lecture 5, rocks become magnetized in a variety of ways. Both igneous and sedimentary rocks can be affected by chemical change, thereby acquiring a secondary magnetization. Many magnetic materials are affected by viscous remanent magnetization. The various components of magnetization sum together to constitute the NRM which is the "raw" remanence of the sample after extraction. The goal of paleomagnetic laboratory work is to isolate the various components of remanence and to ascribe origin, age and reliability to these components. But before the laboratory work can begin, samples must be collected. Sampling strategy is crucial to a successful study. We will briefly describe techniques for sampling, methods of orientation and overall philosophy. We will then turn to an overview of some of the more useful field and laboratory techniques that wind up with an estimate of a paleomagnetic direction.

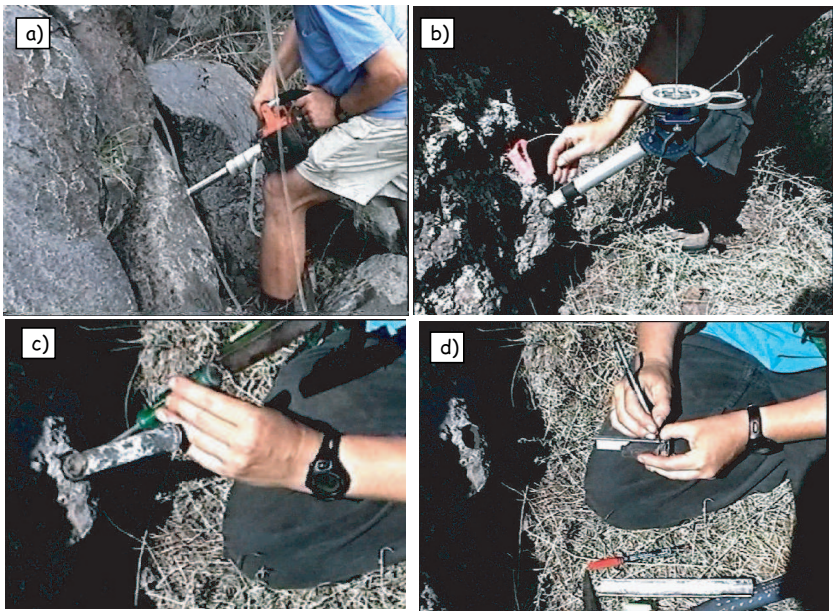

Figure 9.1: Sampling technique with a water-cooled drill: a) drill the sample, b) insert a non-magnetic slotted tube with an adjustable platform around the sample. Rotate the slot to the top of the sample and note the azimuth and plunge of the drill direction (into the outcrop) with a sun and/or magnetic compass and inclinometer. Mark the sample through the slot with a brass or copper wire. c) Extract the sample. d) Make a permanent arrow on the side of the sample in the direction of drill and label the sample with the sample name. Make a note of the name and orientation of the arrow in a field notebook.

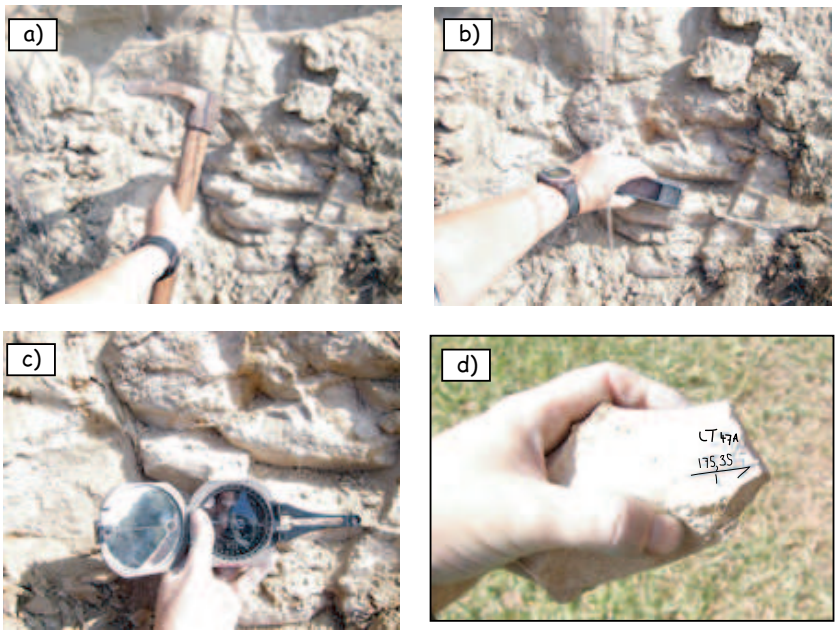

Figure 9.2: Hand sampling technique for soft sediment: a) dig down to fresh material, b) rasp off a flat surface, c) mark the strike and dip on the sample, d) extract the sample and label it.

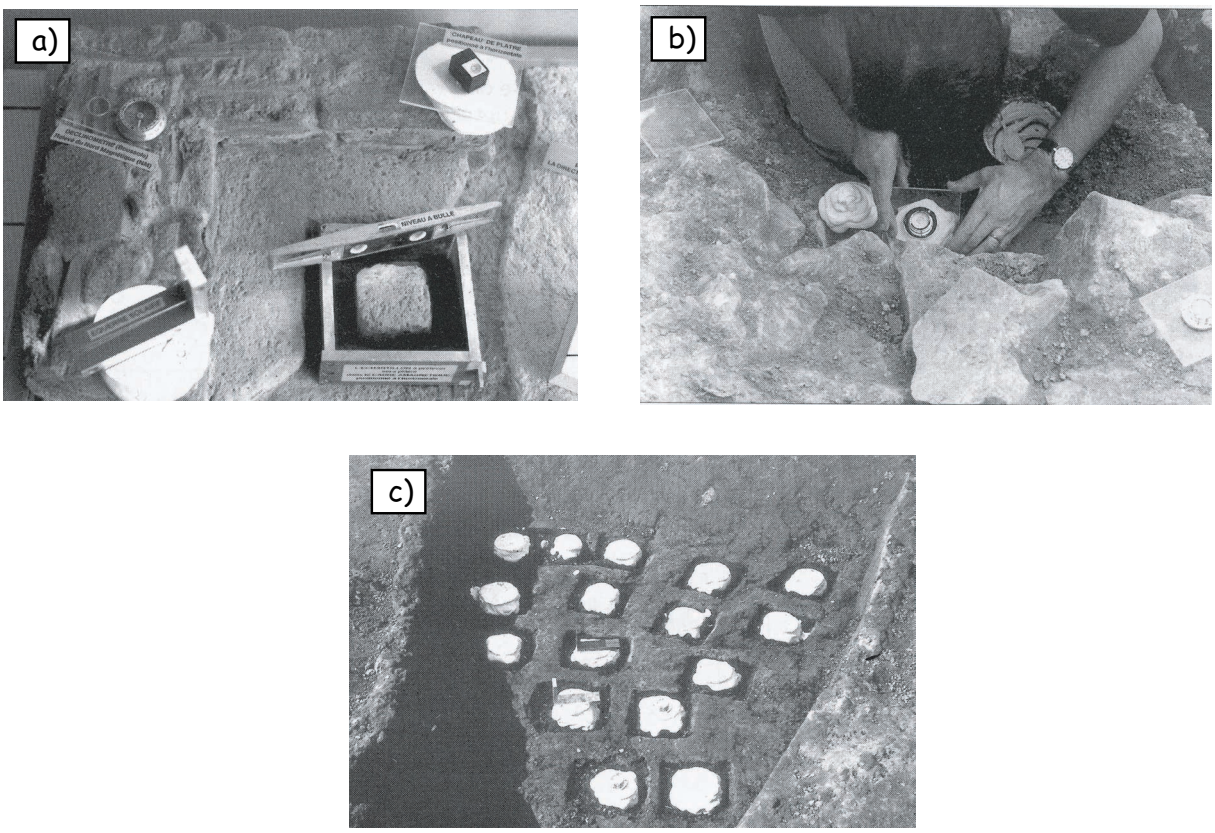

Figure 9.3: Sampling technique for oriented archeological materials. a) cut out a large sample from, for example, a baked hearth. b) cover the sample with non-magnetic plaster of paris. While the plaster of paris is still wet, place a piece of plexiglass on it and orient it such that it is horizontal using a bubble level. c) The direction to magnetic north can be inscribed on the horizontal surface, after the plaster is dry. [Picture from Evin et al. 1998]

9.2 Paleomagnetic sampling

There are several goals in sampling rock units. One is to average out the errors involved in the sampling process itself. Another is to assess the reliability of the recording medium. In addition, we often wish to average the scatter caused by secular variation of the geomagnetic field in order to estimate the time-averaged paleomagnetic field direction representative of the time that the rock unit acquired its magnetization.

The objectives of averaging recording and sampling "noise" are achieved by taking a number N of individually oriented *samples* from a single unit (called a *site*). Samples should be taken such that they represent a single time horizon, that is, they are from a single cooling unit or the same sedimentary horizon. The most careful sample orientation procedure has an uncertainty of several degrees. Precision is gained proportional to $\sqrt{N}$, so to improve the precision, multiple individually oriented samples are required. The number of samples taken should be tailored to the particular project at hand. If one wishes to know polarity, perhaps three samples would be sufficient (these would be taken primarily to assess "recording noise"). If, on the other hand, one wished to make

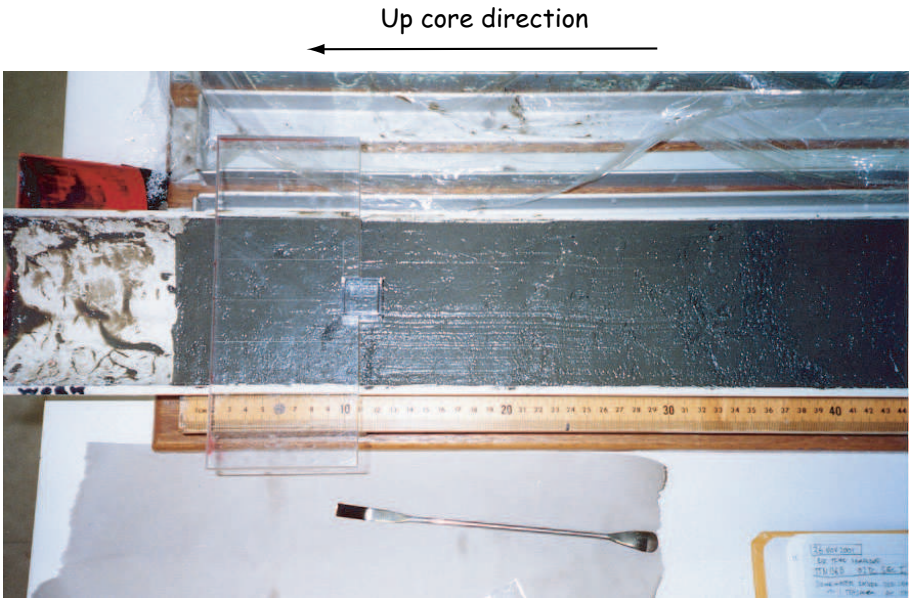

Figure 9.4: Sampling of a sediment core. A plastic cube with a hole in it to let the air escape is pressed into the split surface of a core. The orientation arrow points "up core". After extraction, a label with the sample name is put on. Figure from Kurt Schwehr's web site.

inferences about secular variation of the geomagnetic field, more samples would be necessary to suppress sampling noise.

Some applications in paleomagnetism require that the secular variation of the geomagnetic field (the paleomagnetic "noise") be averaged in order to determine the time-averaged field direction. The geomagnetic field varies with time constants ranging from milliseconds to millions of years. It is a reasonable first order approximation to assume that, when averaged over, say, 100,000 years, the geomagnetic field is similar to that of a geocentric axial dipole (equivalent to the field that would be produced by a bar magnet at the center of the Earth, aligned with the spin axis; see Lecture 2). Thus, when a time-averaged field direction is required, enough sites can be sampled to span sufficient time to achieve this goal. A good rule of thumb is about a hundred sites (each with nine to ten samples), spanning 100,000 years.

Samples can be taken using a gasoline or electric powered drill, as "hand samples" or as "sub-samples" from a piston core. The samples must be oriented before they are removed. There are many ways to orient samples and possible conventions are shown in Figures 9.1, 9.2, 9.3, and 9.4.

If a magnetic compass is used to orient samples in the field. The preferred practice is to set the compass declination to zero. Then, in post-processing, the measured azimuth must be adjusted by the local magnetic declination, which can be calculated from the known reference field (IGRF or DGRF; see Lecture 2). The plunge of the sample can also be gotten using an inclinometer (either with a Pomeroy orientation device as shown in Figure 9.1 or with some other inclinometer, such as that on a Brunton Compass.)

Sometimes large local magnetic anomalies, for example from a strongly magnetized rock unit, can lead to a bias in the magnetic direction that is not compensated for by the IGRF magnetic declination. In such cases, some other means of sample orientation is required. One relatively straightforward way is to use a sun compass. Calculation of a direction using a sun compass is

more involved than for magnetic compass, however. A dial with a vertical needle (a "gnomon") is placed on the horizontal platform shown in Figure 9.5. The angle (α) that the sun's shadow makes with the drilling direction is noted as well as the exact time of sampling and the location of the sampling site. With this information and the aid of the Astronomical Almanac or a simple algorithm (see Appendix), it is possible to calculate the desired direction to reasonable accuracy (the biggest cause of uncertainty is actually reading the shadow angle!).

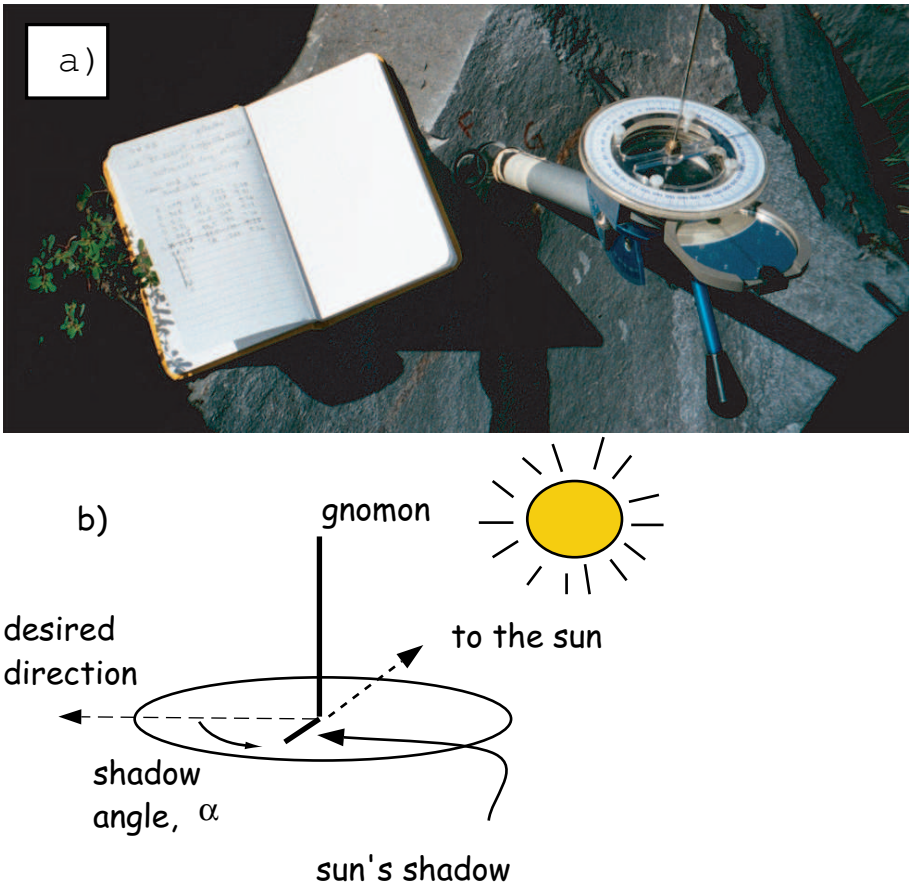

Figure 9.5: a) Pomeroy orientation device in use as a sun compass. b) Schematic of the principles of sun compass orientation.

A new technique, developed by Cathy Constable and Frank Vernon at Scripps Institution of Oceanography (see Figure 9.6) uses differential Global Positioning System (GPS) technology to determine azimuth of a baseline. Two GPS receivers are attached to either end of a one meter non-magnetic rigid base. The location and azimuth of the baseline can be computed from the signals detected by the two receivers. The orientation of the baseline is transferred to the paleomagnetic samples using a laser mounted on the base which is focused on a prism attached to the orientation device used to orient the paleomagnetic samples. The orientations derived by the differential GPS are nearly identical to those obtained by a sun compass, although it takes at least an additional half hour and is rather awkward to transport. Nonetheless, achieving sun-compass accuracy in orientations when the sun is unlikely to be readily available is a major break through for high latitude paleomagnetic field procedures.

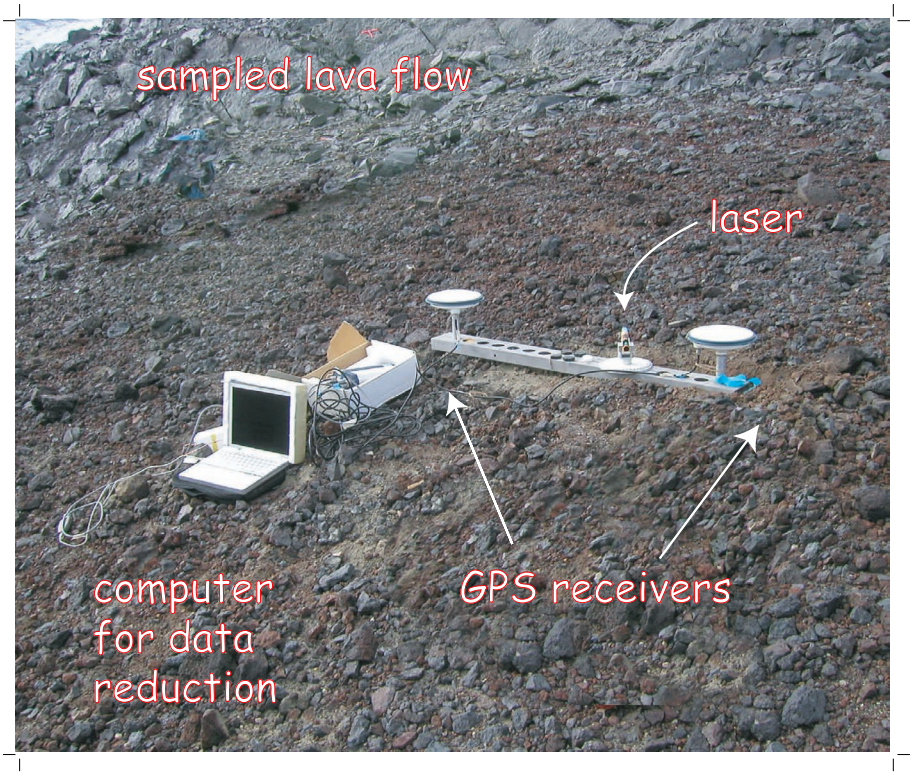

Figure 9.6: Differential GPS system for orienting paleomagnetic samples in polar regions. Photo taken during sampling trip to the foothills of the Royal Society Ranges in Antarctica, Jan. 2004.

9.3 Changing coordinate systems

Samples are brought to the laboratory and trimmed into standard sizes and shapes (see Figure 9.7). These sub-samples are called *paleomagnetic specimens*. Data often must be transformed from the sample coordinate system into, for example, geographic coordinates. This can be done graphically with a stereonet or by means of matrix manipulation. We outline the latter method in the Appendix.

9.4 Measurement of magnetic remanence

We measure the magnetic remanence of paleomagnetic samples in a *magnetometer*, of which there are various types. The cheapest and most readily available are *spinner magnetometers* so named because they spin the sample to create a fluctuating electromotive force (emf). The emf is proportional to the magnetization and can be determined relative to the three axes defined by the sample coordinate system. The magnetization along a given axis is measured by detecting the voltages induced by the spinning magnetic moment within a set of pick-up coils.

Another popular way to measure the magnetization of a sample is to use a *cryogenic magnetometer* (see Figure 9.8). These magnetometers operate using so-called *superconducting quantum interference devices* (SQUIDs). In a SQUID, the flux of an inserted sample is opposed by a current in a loop of superconducting wire. The superconducting loop is constructed with a *weak link* which stops superconducting at some very low current density, corresponding to some very small quantum

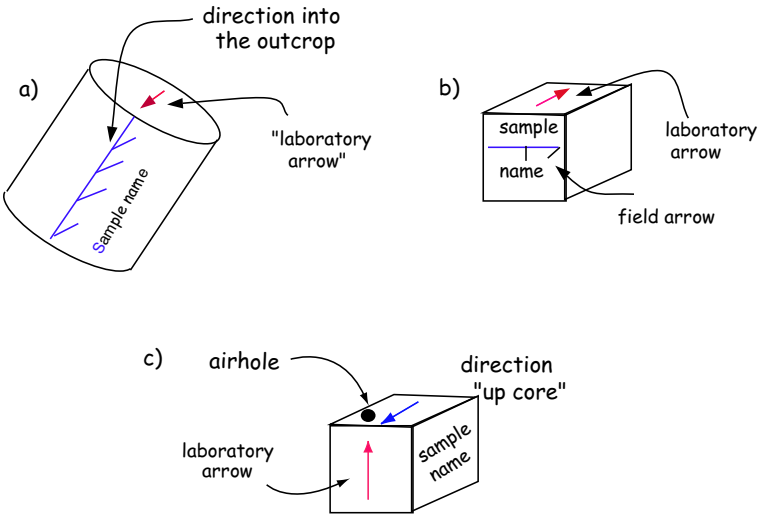

Figure 9.7: Various types of possible sample shapes and orientation conventions. a) A one inch slice from a drilled core. b) A cube of sediment sanded from a hand sample. c) A sample from a piston core.

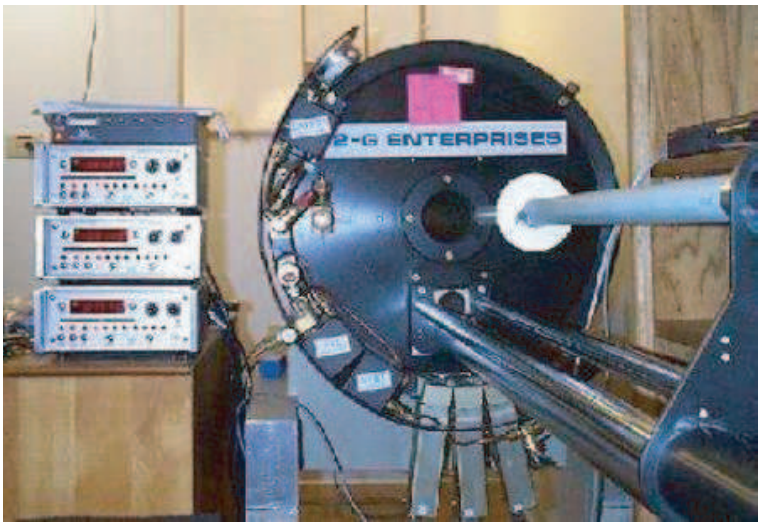

Figure 9.8: a) Cryogenic magnetometer. The sample is inserted into the opening of the shields. There are three SQUIDS that detec the magnetic moment which is read off the three electronic boxes to the left. b) Spinner magnetometer. The sample is inserted into the opening in a cup. It spins around, generating an electromagnetic force which is detected with a circular fluxgate. Two components are measured at a time.

of flux. Thus the flux within the loop can change by discrete quanta. Each incremental change is counted and the total flux is proportional to the magnetization along the axis of the SQUID. Cryogenic magnetometers are much faster and more sensitive than spinner magnetometers, but they cost much more to buy and to operate.

Magnetometers are used to measure the three components of the magnetization necessary to

define a vector (e.g., x_1, x_2, x_3). These data can be converted to the more common form of D, I and M by methods described in Lecture 2.

9.5 Demagnetization techniques

Anyone who has dealt with magnets (including magnetic tape, credit cards, and magnets) knows that they are delicate and likely to demagnetize or change their magnetic properties if abused by heat or stress. Cassette tapes left on the dashboard of the car in the hot sun never sound the same. Credit cards that have been through the dryer may lead to acute embarrassment at the check-out counter. Magnets that have been dropped, do not work as well afterwards. It is not difficult to imagine that rocks that have been left in the hot sun or buried deep in the crust (not to mention altered by diagenesis or bashed with hammers, drills, pick axes, etc.), may not have their original magnetic vectors completely intact. Because rocks often contain millions of tiny magnets, it is possible that some (or all) of these have become realigned, or that they grew since the rock formed. In many cases, there are still grains that carry the original remanent vector, but there are often populations of grains that have acquired new components of magnetization.

Through geologic time, certain grains may acquire sufficient energy to overcome the magnetic anisotropy energy and change their direction of magnetization (Lecture 5). In this way, rocks can acquire a viscous magnetization in the direction of the ambient field. Because the grains that carry the viscous magnetization necessarily have lower magnetic anisotropy energies (they are "softer", magnetically speaking), we expect their contribution to be more easily randomized than the more stable ("harder") grains carrying the ancient remanent magnetization.

There are several laboratory techniques that are available for separating various components of magnetization. Paleomagnetists rely on the relationship of relaxation time, coercivity, and temperature in order to remove (*demagnetize*) low stability remanence components. The fundamental principle that underlies demagnetization techniques is that the lower the relaxation time τ, the more likely the grain will carry a secondary magnetization. The basis for *alternating field* (AF) demagnetization is that components with short relaxation times also have low coercivities. The basis for *thermal* demagnetization is that these grains also have low blocking temperatures.

In AF demagnetization (see Figure 9.9a), an oscillating field is applied to a paleomagnetic sample in a null magnetic field environment. All the grain moments with coercivities below the peak AF will track the field. These entrained moments will become stuck as the peak field gradually decays below the coercivities of individual grains. Assuming that there is a range of coercivities in the sample, the low stability grains will be stuck half along one direction of the AF and half along the other direction; the net contribution to the remanence will be zero. In practice, we demagnetize samples sequentially along three orthogonal axes, or while "tumbling" the sample around three axes during demagnetization.

Thermal demagnetization (see Figure 9.9b) exploits the relationship of relaxation time and temperature. There will be a temperature below the curie temperature at which the relaxation time is a few hundred seconds. When heated to this temperature, grains with relaxation times this short will be in equilibrium with the field. This is the *unblocking temperature*. If the external field is zero, then there will be no net magnetization. Lowering the temperature back to room temperature will result in the relaxation times growing exponentially until these moments are once again fixed. In this way, the contribution of lower stability grains to the NRM can be randomized. Alternatively, if there is a DC field applied during cooling, the grains whose unblocking temperatures has been

a)

b)

Figure 9.9: a) Alternating field demagnetizer. The sample is placed within the coil inside the tubular shield. An alternating field is generated with a specified peak intensity. This decays away, randomizing all magnetic moments that are softer than the peak field that have a component parallel to the applied field direction. The procedure is repeated along all three axis. A small DC field can applied along the direction of the coils to produce an ARM. b) Thermal demagnetizer. Samples are placed in boats inside a non-inductively wound oven that is inside the tubular shields. The ovens are heated to a specified temperature and allowed to cool either in zero field or in a laboratory controlled DC field produced by a coil inside the shield. This either demagnetizes or remagnetizes all grains with blocking temperatures lower than the specified temperature.

exceeded will be realigned in the new field direction; they will have acquired a partial thermal remanent magnetization (pTRM).

We sketch the principles of progressive demagnetization in Figure 9.10. Initially, the NRM is the sum of two components carried by populations with different coercivities. The distributions of coercivities are shown in the histograms to the left in Figure 9.10. Two components of magnetization are shown as heavy lines in the plots to the right. In these examples, the two components are orthogonal. The sum of the two components at the start (the NRM) is shown as a + on the vector plots to the right. After the first AF demagnetization step, the contribution of the lowest coercivity grains has been erased and the remanence vector moves to the position of the first dot away from the +. Increasing the AF gradually eats away at the remanence vectors (shown as dashed arrows and dots in the plots to the right) which eventually approach the origin.

There are four different sets of coercivity spectra shown in Figure 9.10, each with a distinctive behavior during demagnetization. If the two coercivity fractions are completely distinct, the two components are clearly defined (Figure 9.10a) by the progressive demagnetization. If there is some overlap in the coercivity distribution of the components the resulting demagnetization diagram is curved (Figure 9.10b). If the two components completely overlap, both components are removed simultaneously and an apparently single component demagnetization diagram may result (Figure 9.10c). It is also possible for one coercivity spectrum to include another as shown in Figure 9.10d. Such cases result in "S" shaped demagnetization curves. Because complete overlap actually happens in "real" rocks, it is desirable to perform both AF and thermal demagnetization. If the two components overlap completely in coercivity, they might not have overlapping blocking

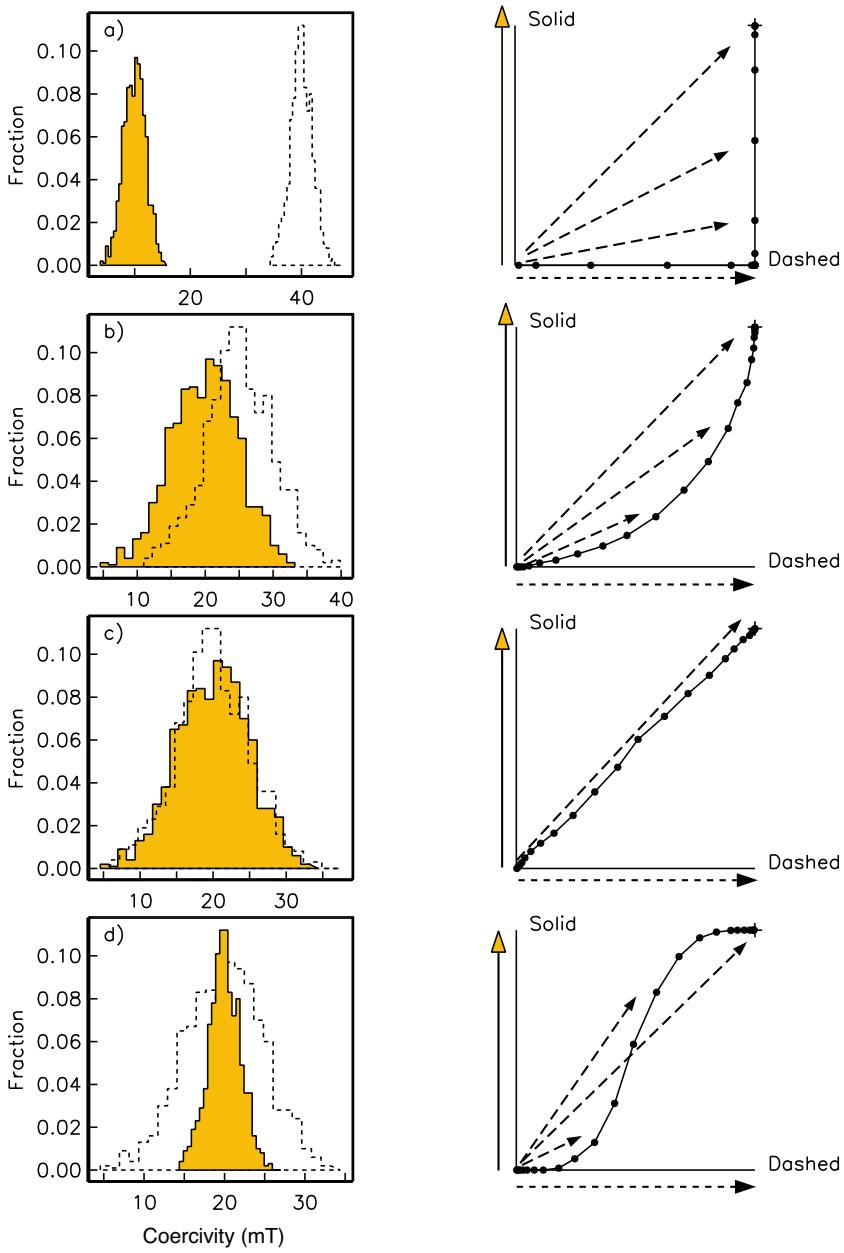

Figure 9.10: Principle of progressive demagnetization. Specimens with two components of magnetization (shown by heavy arrows on the right hand side), with discrete coercivities (plotted as histograms to the left). The original "NRM" is the sum of the two magnetic components and is shown as the + in the diagrams to the right. Successive demagnetization steps remove the component with coercivities lower than the peak field, and the NRM vector changes as a result. a) The two distributions of coercivity are completely separate. b) The two distributions partially overlap resulting in simultaneous removal of both components. c) The two distributions completely overlap. d) One distribution envelopes the other.

temperature distributions and vice versa. It is unlikely that samples from the same lithology will all have identical overlapping distributions, so multiple samples can provide clues to the possibility of completely overlapped directions in a given sample.

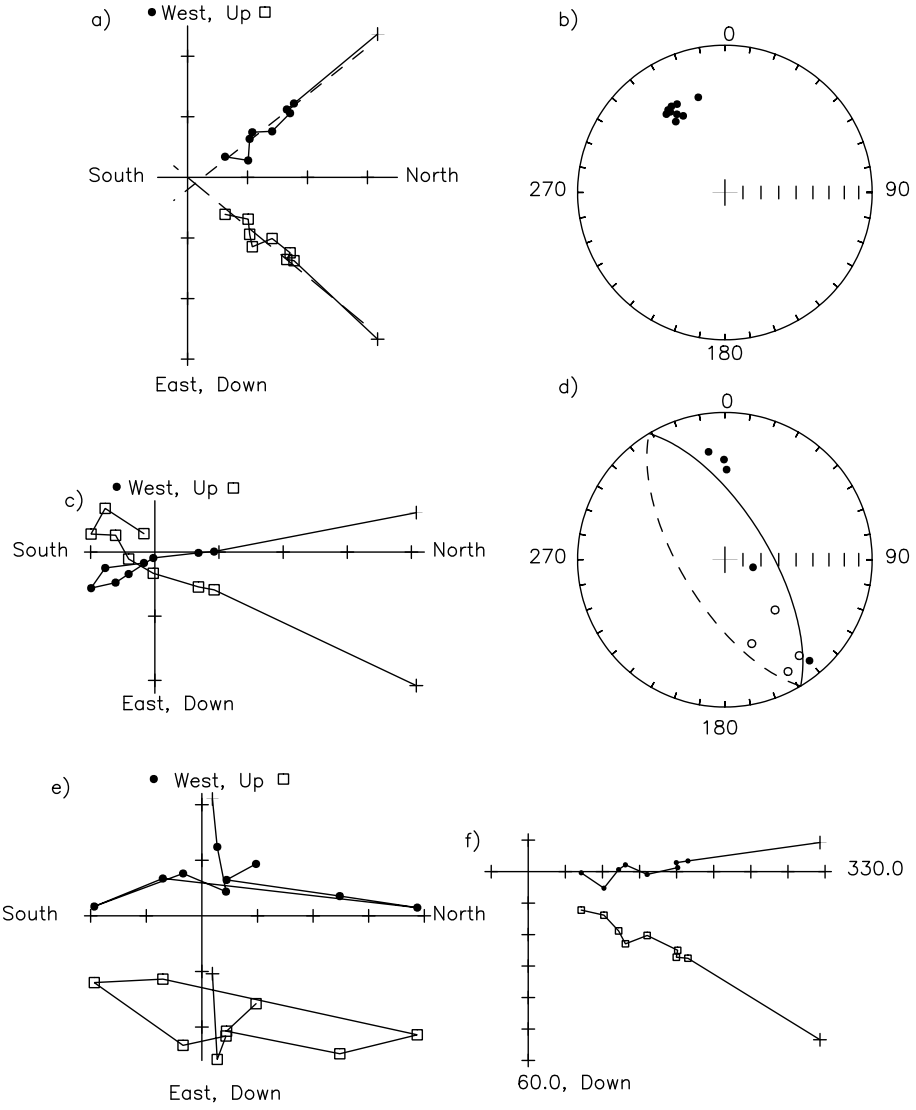

Figure 9.11: a) Orthogonal projection of data plotted with North on the horizontal axis. A single component of magnetization is present (see text). The horizontal projection is plotted with solid symbols and the vertical (North-down) component is plotted with open squares. The best-fit line through the data, as calculated by principal component analysis, is shown as a dashed line. b) Same data as in a), but plotted on an equal area projection. Solid (open) symbols are projections onto the lower (upper) hemisphere. c) Sample with two components that have overlapping stabilities. d) Same data as in c), but in an equal area projection. The trace of the best-fitting plane is shown, with a solid (dashed) line being a projection onto the lower (upper) hemisphere. e) Example of a complicated multi-component sample. f) Data from a) replotted with the horizontal axis along 330° instead of with respect to North.

9.6 Estimating a direction from demagnetization data

Now we will consider briefly the issue of what to do with the demagnetization data in terms of display and estimating a best-fit direction for various components.

The standard practice in demagnetization is to measure the NRM and then to subject the sample to a series of demagnetization steps of increasing severity using the equipment described earlier in the lecture. The magnetization of the sample is measured after each step. During demagnetization, the remanent magnetization vector will change until the most stable component has been isolated, at which point the vector decays in a straight line to the origin. This final component is called the *characteristic remanent magnetization* or ChRM.

Visualizing demagnetization data is a three-dimensional problem and therefore difficult to plot on paper. Paleomagnetists often rely on a set of two projections of the vectors, one on the horizontal plane and one on the vertical plane. These are variously called Zijderveld diagrams (Zijderveld [1967]), orthogonal projections, or vector end-point diagrams.

In orthogonal projections, the North component (x_1) is plotted versus East (x_2) (solid symbols) in one projection, and North (x_1) is replotted versus Down (x_3) (open symbols) in another projection. Here, paleomagnetic convention differs from the usual x-y plotting convention because x_2 and x_3 are on the $-y$ axis. The paleomagnetic conventions make sense if one visualizes the diagram as a map view for the solid symbols and a vertical projection for the open symbols. It may be advantageous to plot North on the vertical axis and East positive to the right. In this case the vertical projection is East versus Down. This projection is useful if the magnetization is more East-West than North-South. In fact, the horizontal axis can be any direction within the horizontal plane.

In Figure 9.11, we show three general types of demagnetization behavior. In Figure 9.11a-b, the sample has a North-Northwest and downward directed NRM (plotted as +'s). The direction does not change during demagnetization and the NRM is a single vector. The directional data are also plotted on the equal area net to the right (Figure 9.11b) and fall in the NW quadrant of the lower hemisphere. The sample in Figure 9.11c shows a progressive change in direction from a North-Northwest and downward directed component to a South-Southeast and upward direction. The vector continuously changes direction to the end and no final "clean" direction has been confidently isolated. These data are plotted on an equal area projection to the right (Figure 9.11d) along with the trace of the best-fitting plane (a great circle). The most stable component probably lies somewhere near the best-fitting plane.

In Figure 9.11e, we show what is informally known as a "spaghetti" diagram. The NRM switches from direction to direction, with little coherence from step to step. Such data are difficult to interpret and are usually thrown out.

Some people choose to plot the pairs of points (x_1, x_2) versus (H, x_3) where H is the horizontal projection of the vector given by $\sqrt{x_1^2 + x_2^2}$. In this projection, which is sometimes called a *component plot*, the two axes do not correspond to the same vector from point to point. Instead, the coordinate system changes with every demagnetization step because H almost always changes direction, even if only slightly. Plotting H versus x_3 is therefore a confusing and misleading practice. The primary rationale for doing so is because, in the traditional orthogonal projection, the vertical component reveals only an apparent inclination. If something close to true inclination is desired, then, instead of plotting H and x_3, one can simply rotate the horizontal axes of the orthogonal plot such that it closely parallels the desired declination (Figure 9.11f).

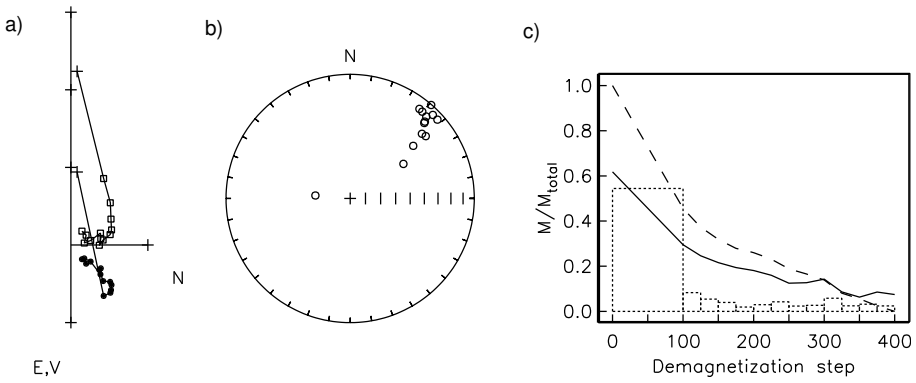

Figure 9.12: a) Specimen with strongly overlapping remanence components, in an orthogonal projection. b) Same data as in a) plotted on an equal area projection. c) Decay of NRM intensity during the demagnetization procedure (solid line). The dashed line is the decay of the vector difference sum. Boxes represent the intensity removed after each step.

9.7 Vector difference sum

An equal area projection may be the most useful way to present demagnetization data from a sample with several strongly overlapping remanence components (such as in Figures 9.11c-d and 9.12). In order to represent the vector nature of paleomagnetic data, it is necessary to plot intensity information. Intensity can be plotted versus demagnetization step in an *intensity decay curve* (Figure 9.12c). However, if there are several components with different directions, the intensity decay curve cannot be used to determine, say, the blocking temperature spectrum, because it is the vector sum of the two components. It is therefore advantageous to consider the decay curve of the *vector difference sum* (VDS.) The VDS "straightens out" the various components by summing up the vector differences at each demagnetization step, so the total magnetization is plotted, as opposed to the resultant (see Figure 9.12).

9.8 Best-fit lines and planes

Orthogonal vector projections aid in identification of the various remanence components in a sample. Demagnetization data are usually treated using what is known as *principal component analysis* (Kirschvink [1980]). What comes out of the analysis is a best-fit line through straight-line, single component data as in Figure 9.11a,b or a best-fit planes or great circle through multi-component data as in Figure 9.11c,d, and the "maximum angle of deviation" (MAD) for each of these. The details of the analysis are given in the Appendix.

9.9 Field strategies

In addition to establishing that a given rock unit retains a consistent magnetization, it is also of interest to establish when this magnetization was acquired. Arguments concerning the age of magnetic remanence can be built on indirect petrographic evidence as to the relative ages of various magnetic minerals, or by evidence based on geometric relationships in the field. There are two key field tests that require special sampling strategies: the fold test and the conglomerate test.

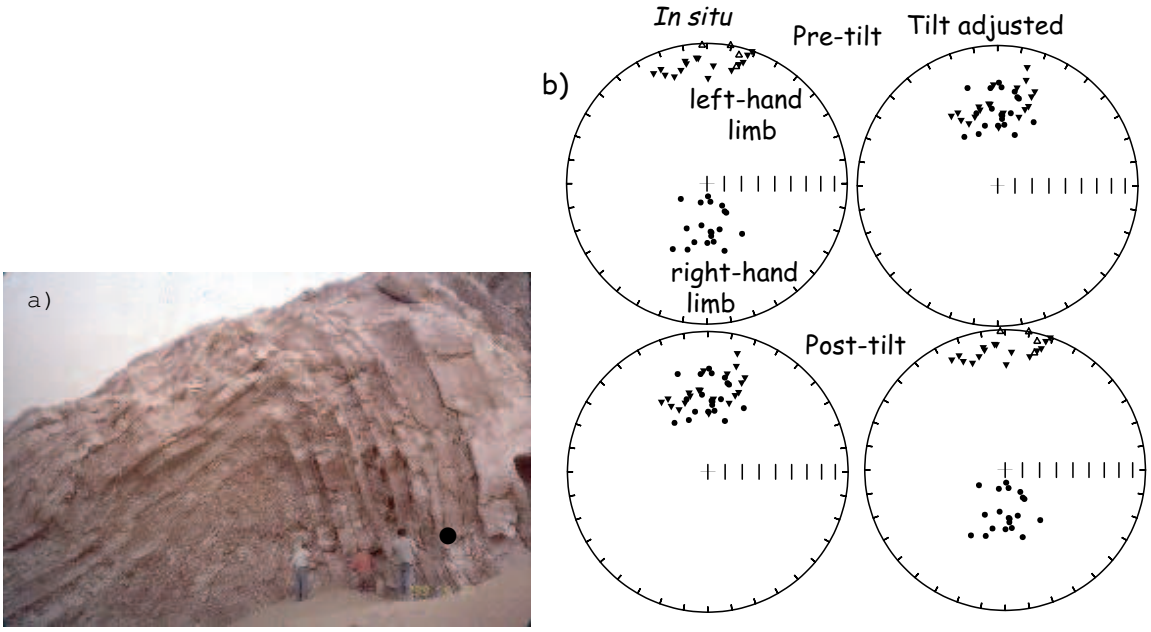

Figure 9.13: Sampling units with different bedding attitudes in the "fold test". a) Example of folded beds. (Picture from Dupont-Nivet et al., 2002.) b) Hypothetical paleomagnetic directions are shown on equal area projections before and after adjusting for bedding tilt. Top pair represents the case in which the grouping of paleomagnetic directions is improved after adjusting for tilt which would argue for a pre-tilt acquisition of remanence. Lower pair represents a post-tilt acquisition of remanence in which the grouping is worse after restoring beds to the horizontal position.

The *fold test* relies on the tilting or folding of the target geological material. If, for example, one wanted to establish the antiquity of a particular set of directions, one could deliberately sample units of like lithology, with different present attitudes (Figure 9.13). If the recovered directions are more tightly grouped before adjusting for tilt (as in the lower left panel), then the magnetization is likely to have been acquired after tilting. On the other hand, if directions become better grouped in the tilt adjusted coordinates (see upper right panel), one has an argument in favor of a pre-tilt age of the magnetization. Methods for quantifying the tightness of grouping in various coordinate systems will be discussed in later lectures.

In the *conglomerate test*, lithologies that are desirable for paleomagnetic purposes must be found in a conglomerate bed (Figure 9.14). In this rare and happy circumstance, we can sample them and show that: 1) the rock magnetic behavior is the same for the conglomerate samples as for those being used in the paleomagnetic study, 2) the directions of the studied lithology are well grouped, (Figure 9.14) and 3) the directions from the conglomerate clasts are randomly oriented (see Figure 9.14). If the directions of the clasts are not randomly distributed (Figure 9.14), then presumably the conglomerate clasts (and, by inference, the paleomagnetic samples from the studied lithology as well) were magnetized after deposition of the conglomerate. We will discuss statistical methods for deciding if a set of directions is random in later lectures.

The *baked contact test* is illustrated in Figure 9.15. It is similar to the conglomerate test in that we seek to determine whether the lithology in question has undergone pervasive secondary overprinting. When an igneous body intrudes into an existing *host rock*, it heats (or bakes) the

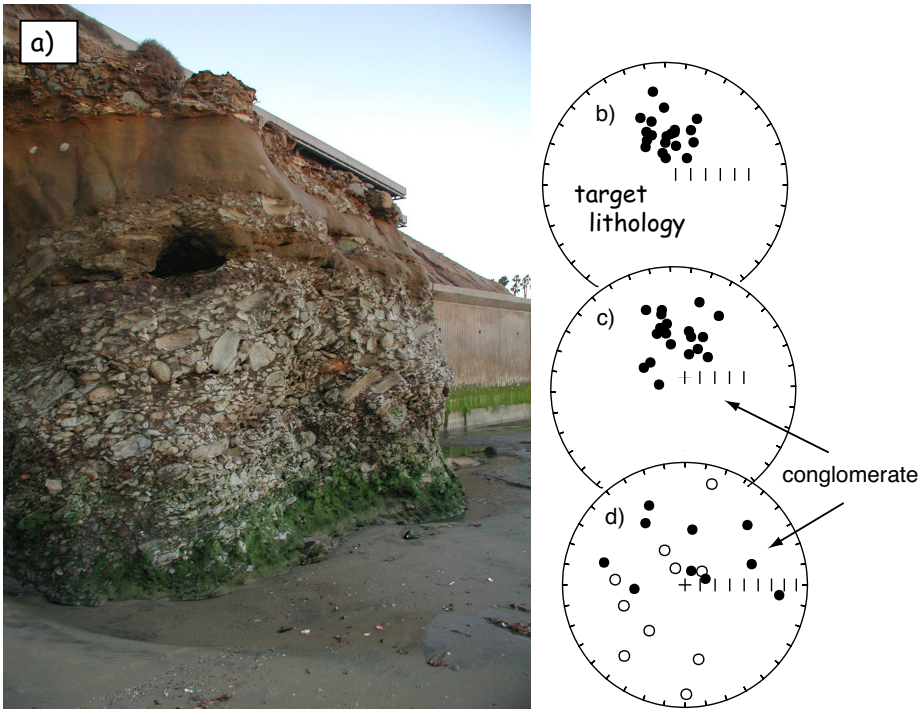

Figure 9.14: The paleomagnetic conglomerate test. a) The target lithology was involved in a catastrophic event leading to incorporation into a conglomerate bed. Samples are taken from individual clasts. The directions of samples from the target lithology are shown in b) indicating that it is relatively homogeneously magnetized. c) dirctions from the conglomerate clasts are also homogeneously magnetized; the magnetization must post-date formation of the conglomerate. In a positive conglomerate test d), the magnetization vectors of samples from the conglomerate clasts are random.

contact zone to above the Curie temperature of the host rock. The baked contact immediately adjacent to the intrusion should therefore have the same remanence direction as the intrusive unit. This magnetization may be in an entirely different direction from the pre-existing host rock. The maximum temperature reached in the baked zone decreases away from the intrusion and remagnetization is not complete. Thus the NRM directions of the baked zone gradually change from that of the intrusion to that of the host rock. Such a condition would argue against pervasive overprinting in the host rock that post-dated the intrusion, and the age of the intrusion would provide an upper bound on the age of remanence in the host rock.

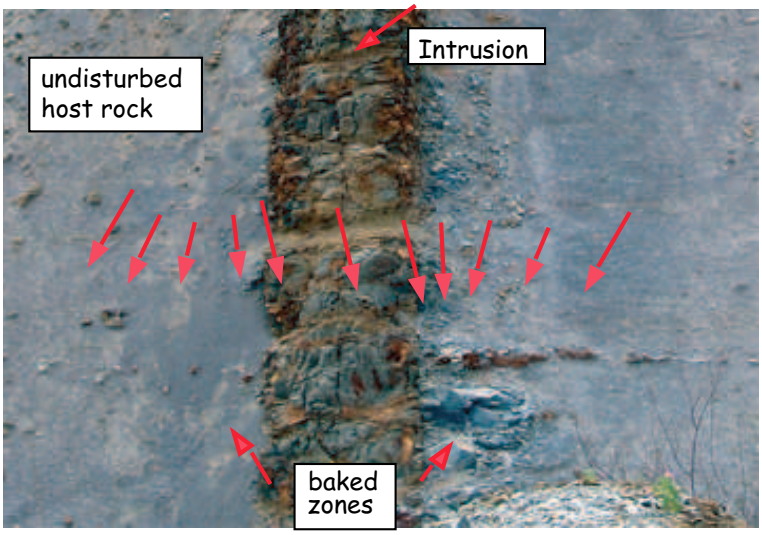

Figure 9.15: The baked contact test. In a positive test, zones baked by the intrusion are remagnetized and have directions that grade from that of the intrusion to that of the host rock. If all the material is homogeneously magnetized, then the age of the intrusion places an upper bound on the age of magnetization.

Appendix

A Directions using a sun compass

Referring to Figure 9.5, we see that the azimuth of the desired direction is the direction of the of the shadow plus the shadow angle α. The declination of the shadow itself is 180° from the direction toward the sun. In Figure A1, the problem of calculating declination from sun compass information is set up as a spherical trigonometry problem, similar to those introduced in Lecture 2 and its appendix. The declination of the shadow direction β', is given by 180 - β. We also know the latitude of the sampling location L (λ_L). We need to calculate the latitude of S (the point on the Earth's surface where the sun is directly overhead), and the local hour angle H.

Knowing the time of observation (in Universal Time), the position of S ($\lambda_s = \delta, \phi_s$ in Figure A1) can be calculated with reasonable precision (to within 0.01°) for the period of time between 1950 and 2050 using the procedure recommended in the 1996 Astronomical Almanac:

- First, calculate the Julian Day J. Then, calculate the fraction of the day in Universal Time U. Finally, calculate the parameter d which is the number of days from J2000 by:

$$d = J - 2451545 + U.$$

- The mean longitude of the sun (ϕ_s), corrected for aberration, can be estimated in degrees by:

$$\phi_s = 280.461 + 0.9856474d.$$

- The mean anomaly $g = 357.528 + 0.9856003d$ (in degrees).
- Put ϕ_s and g in the range $0 \rightarrow 360°$.
- The longitude of the ecliptic is given by $\phi_E = \phi_s + 1.915 \sin g + 0.020 \sin 2g$ (in degrees).
- The obliquity of the ecliptic is given by $\epsilon = 23.439 - 0.0000004d$.
- Calculate the right ascension (A) by:

$$A = \phi_E - ft \sin 2\phi_E + (f/2)t^2 \sin 4\phi_E,$$

where $f = 180/\pi$ and $t = \tan^2\epsilon/2$.

- The so-called "declination" of the sun (δ in Figure A1 which should not be confused with the magnetic declination D), which we will use as the latitude λ_s, is given by:

$$\delta = \sin^{-1}(\sin\epsilon \sin\phi_e).$$

- Finally, the equation of time in degrees is given by $E = 4(\phi_s - A)$.

We can now calculate the Greenwich Hour Angle GHA from the Universal Time U (in minutes) by $GHA = (U + E)/4 + 180$. The local hour angle (H in Figure A1) is $GHA + \phi_L$. We calculate β using the laws of spherical trigonometry (see Appendix to Lecture 2). First we calculate θ by the Law of Cosines (remembering that the cosine of the colatitude equals the sine of the latitude):

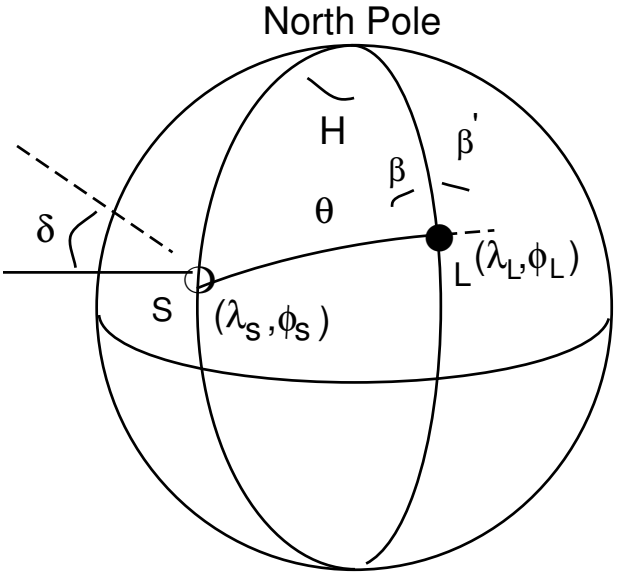

Figure A1: Calculation of the azimuth of the shadow direction (β') relative to true North, using a sun compass. L is the site location (at λ_L, ϕ_L), S is the position on the Earth where the sun is directly overhead (λ_S, ϕ_S).

$$\cos\theta = \sin\lambda_L \sin\lambda_s + \cos\lambda_L \cos, \lambda_s \cos H$$

and finally using the Law of Sines:

$$\sin\beta = (\cos\lambda_s \sin H)/\sin\theta.$$

If $\lambda_s < \lambda_L$, then the required angle is the shadow direction β', given by: $\beta' = 180 - \beta$. The azimuth of the desired direction in Figure 9.5 is β' plus the measured shadow angle α.

B Transformation of coordinates

The sample coordinate system is defined by a right-hand rule where the thumb ($\mathbf{X}_1$) is directed parallel to an arrow marked on the sample, the index finger ($\mathbf{X}_2$) is in the same plane but at right angles and clockwise to $\mathbf{X}_1$ and the middle finger ($\mathbf{X}_3$) is perpendicular to the other two (Figure B1a). The transformation of coordinates (x_i) from the $\mathbf{X}_i$ axes to the coordinates in the desired $\mathbf{X}'$ coordinate system (x'_i) is done by $x'_i = a_{ij}x_j$, or:

$$\begin{pmatrix} x'_1 \\ x'_2 \\ x'_3 \end{pmatrix} = \begin{pmatrix} a_{11} & a_{12} & a_{13} \\ a_{21} & a_{22} & a_{23} \\ a_{31} & a_{32} & a_{33} \end{pmatrix} \begin{pmatrix} x_1 \\ x_2 \\ x_3 \end{pmatrix}, \tag{B1}$$

where the a_{ij} are the *direction cosines* (the cosines of the angles between the different axes), where the subscript i refers to the new coordinate system $\mathbf{X}'$ and the subscript j refers to the old $\mathbf{X}$ coordinates. Thus, a_{12} is the cosine of the angle between $\mathbf{X}'_1$ and $\mathbf{X}_2$. The various a_{ij} can be calculated using spherical trigonometry (Lecture 2). For example, a_{11} for the general case depicted

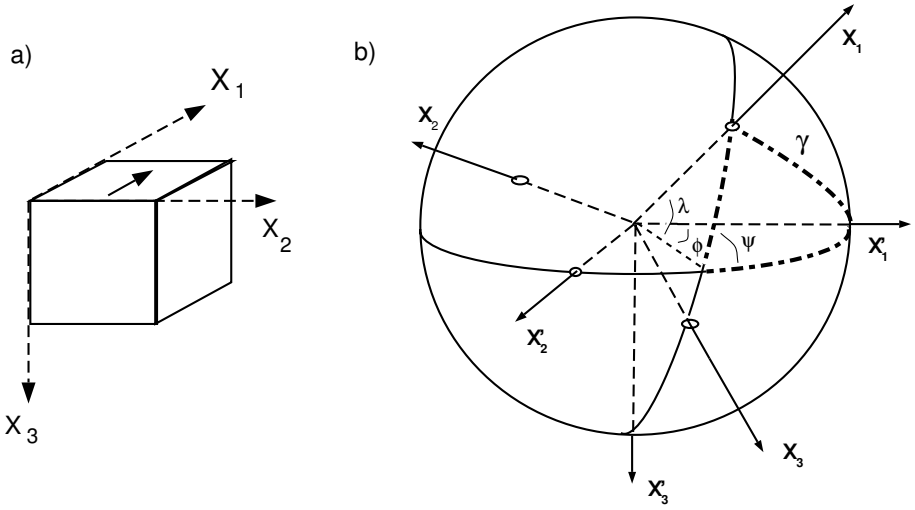

Figure B1: a) Sample coordinate system. b) Trigonometric relations between two cartesian coordinate systems, $\mathbf{X}_i$ and $\mathbf{X}'_i$. λ, ϕ, ψ are all known and the angles between the various axes can be calculated using spherical trigonometry. For example, the angle γ between $\mathbf{X}_1$ and $\mathbf{X}'_1$ forms one side of the triangle shown by dash-dot lines. Thus, $\cos\gamma = \cos\lambda\cos\phi + \sin\lambda\sin\phi\cos\psi$.

in Figure B1 is $\cos\alpha$, which is given by the Law of Cosines (Lecture 2) by using appropriate values, or:

$$\cos\alpha = \cos\lambda\cos\phi + \sin\lambda\sin\phi\cos\psi.$$

The other a_{ij} can be calculated in a similar manner. In the case of most coordinate system rotations used in paleomagnetism, X_2 is in the same plane as X'_1 and X'_2 (and is horizontal) so $\psi = 90°$. This problem is much simpler. The directions cosines for the case where $\psi = 90$ are:

$$a = \begin{pmatrix} \cos\lambda\cos\phi & -\sin\phi & -\sin\lambda\cos\phi \\ \cos\lambda\sin\phi & \cos\phi & -\sin\lambda\sin\phi \\ \sin\lambda & 0 & \cos\lambda \end{pmatrix}. \tag{B2}$$

The new coordinates can be obtained from equation B1, as follows:

$$\begin{aligned} x'_1 &= a_{11}x_1 + a_{12}x_2 + a_{13}x_3 \\ x'_2 &= a_{21}x_1 + a_{22}x_2 + a_{23}x_3 \\ x'_3 &= a_{31}x_1 + a_{32}x_2 + a_{33}x_3. \end{aligned} \tag{B3}$$

The declination and inclination can be calculated by inserting these values in the equations in Lecture 2 and its appendix. In practice, there are two transformations that are routinely made in paleomagnetism. Magnetizations are measured in sample coordinates. First, they must then be rotated into geographic coordinates. For this, the azimuth and plunge of the sample $\mathbf{X}_1$ axis can be used for ϕ and λ, respectively in equations B2 and B3. Second, samples are often taken from geologic units that are no longer in the same position as when they were magnetized; they are tilted. If paleo-horizontal can be recognized, for example, from quasi-horizontal laminations in sedimentary rocks, the orientation of the bedding plane can be measured as *strike* and *dip*, or as dip and *dip direction*. The strike is the direction of a horizontal line within the bedding plane and the

dip is the angle that the plane makes with the horizontal. Our convention is that dip is measured to the "right" of the strike direction. If the direction cosines relating the dip and dip direction to the geographic coordinate systems are plugged in for the a_{ij}, the data can be transformed into so-called *tilt adjusted* coordinates using equation B3.

C Principal Component Analysis

A sequence of data points which form a single component are equally weighted. The D, I, and M data are converted to corresponding x values (see Lecture 2). Then we calculate the coordinates of the "center of mass" ($\bar{x}$) of the data points:

$$\bar{x}_1 = \frac{1}{N}(\sum_1^N x_{1i}); \quad \bar{x}_2 = \frac{1}{N}(\sum_1^N x_{2i}); \quad \bar{x}_3 = \frac{1}{N}(\sum_1^N x_{3i}), \tag{C1}$$

where N is the number of data points involved. We then transform the origin of the data cluster to the center of mass:

$$x'_{1i} = x_{1i} - \bar{x}_1; \quad x'_{2i} = x_{2i} - \bar{x}_2; \quad x'_{3i} = x_{3i} - \bar{x}_3, \tag{C2}$$

where x'_i are the transformed coordinates.

C1 The orientation tensor and eigenvector analysis

The *orientation tensor* $\mathbf{T}$ (Scheidegger [1965]) (also known as the matrix of sums of squares and products), is extremely useful in paleomagnetism:

$$\mathbf{T} = \begin{pmatrix} \sum x'_{1i}x'_{1i} & \sum x'_{1i}x_{2i} & \sum x'_{1i}x'_{3i} \\ \sum x'_{1i}x'_{2i} & \sum x'_{2i}x'_{2i} & \sum x'_{2i}x'_{3i} \\ \sum x'_{1i}x'_{3i} & \sum x'_{2i}x'_{3i} & \sum x'_{3i}x'_{3i} \end{pmatrix}. \tag{C3}$$

$\mathbf{T}$ is a 3 x 3 matrix, where only six of the nine elements are independent. It is constructed in some coordinate system, such as the geographic or sample coordinate system. Usually, none of the six independent elements are zero. There exists, however, a coordinate system along which the "off-axis" terms are zero and the axes of this coordinate system are called the *eigenvectors* of the matrix. The three elements of $\mathbf{T}$ in the eigenvector coordinate system are called *eigenvalues*. In terms of linear algebra, this idea can be expressed as:

$$\mathbf{TV} = \tau\mathbf{V}, \tag{C4}$$

where $\mathbf{V}$ is the matrix containing three *eigenvectors* and τ is the diagonal matrix containing three *eigenvalues*. Equation C4 is only true if:

$$\det|\mathbf{T} - \tau| = 0. \tag{C5}$$

If equation C5 is expanded, we have a third degree polynomial whose roots (τ) are the eigenvalues:

$$(T_{11} - \tau)[(T_{22} - \tau)(T_{33} - \tau) - T_{23}^2] -$$

$$T_{12}[T_{12}(T_{33}-\tau)-T_{13}T_{23}]+T_{13}[T_{13}T_{23}-T_{13}(T_{22}-\tau)]=0.$$

The three possible values of τ (τ_1, τ_2, τ_3) can be found with iteration and determination. In practice, there are many programs for calculating τ. My personal favorite is the Numerical Module for Python (see many free web sites, especially Scientific Python (SciPy) for hints. Please note that the conventions adopted here are to scale the τ's such that they sum to one; the largest eigenvalue is termed τ_1 and corresponds to the eigenvector $\mathbf{V}_1$.

C2 Principal components of the orientation matrix

Inserting the values for the transformed components calculated in equation C2 into $\mathbf{T}$ gives the covariance matrix for the demagnetization data. The direction of the axis associated with the greatest scatter in the data (the principal eigenvector $\mathbf{V}_1$) corresponds to a best-fit line through the data. This is usually taken to be the direction of the component in question. This direction also corresponds to the axis around which the "moment of inertia" is least. The eigenvalues of $\mathbf{T}$ are the variances associated with each eigenvector. Thus the standard deviations are $\sigma_i = \sqrt{\tau_i}$. The so-called *maximum angular deviation* or MAD of Kirschvink [1980] is defined as:

$$MAD = \tan^{-1}(\sqrt{(\sigma_2^2+\sigma_3^2)}/\sigma_1). \quad \text{(C6)}$$

If no unique principal direction can be isolated (as for the sample in Figure 9.11c-d), the eigenvector $\mathbf{V}_3$ associated with the least eigenvalue τ_3 can be taken as the pole to the best-fit plane wherein the component of interest must lie. Kirschvink [1980] also defines a MAD angle for the plane as:

$$MAD_{\text{plane}} = \tan^{-1}\sqrt{\tau_3/\tau_2+\tau_3/\tau_1}.$$

Bibliography

Butler, R. F. (1992), *Paleomagnetism: Magnetic Domains to Geologic Terranes*, Blackwell Scientific Publications.

Collinson, D. W. (1983), 'Methods in Rock Magnetism and Paleomagnetism'.

Dupont-Nivet, G., Guo, Z., Butler, R. & Jia, C. (2002), 'Discordant paleomagnetic direction in Miocene rocks from the central Tarim Basin: evidence for local deformation and inclination shallowing', *Earth Planet. Sci. Lett.* **199**, 473–482.

Evin, K., Lambert, G.-N., Langouët, L., Lanos, P. & Oberlin, C. (1998), *La datation en laboratororie*, Editions Errance, Paris.

Kirschvink, J. L. (1980), 'The least-squares line and plane and the analysis of paleomagnetic data', *Geophys. Jour. Roy. Astron. Soc.* **62**, 699–718.

Scheidegger, A. E. (1965), 'On the statistics of the orientation of bedding planes, grain axes, and similar sedimentological data', *U.S. Geo. Surv. Prof. Pap.* **525-C**, 164–167.

Zijderveld, J. D. A., ed. (1967), *A.C. demagnetization of rocks: analysis of results*, Methods in Paleomagnetism, Chapman and Hall.